STEM CELLS AND DEVELOPMENT
Volume 30, Number 9, 2021

DOI: 10.1089/scd.2020.0190

Downregulation of SUV39H1 and CITED2 Exerts Additive Effect on Promoting Adipogenic Commitment of Human Mesenchymal Stem Cells

Lun Tan, Linh Tran, Stephanie Ferreyra, Jose A. Moran, Zachary Skovgaard, Amparo Trujillo, Esra ibili, and Yuanxiang Zhao

Human adipogenesis is the process through which uncommitted human mesenchymal stem cells (hMSCs) differentiate into adipocytes. Through a *siRNA*-based high-throughput screen that identifies adipogenic regulators whose expression knockdown leads to enhanced adipogenic differentiation of hMSCs, two new regulators, SUV39H1, a histone methyltransferase that catalyzes H3K9Me3, and CITED2, a CBP/p300-interacting transactivator with Glu/Asp-rich carboxy-terminal domain 2 were uncovered. Both SUV39H1 and CITED2 are normally downregulated during adipogenic differentiation of hMSCs. Further expression knockdown induced by *siSUV39H1* or *siCITED2* at the adipogenic initiation stage significantly enhanced adipogenic differentiation of hMSCs as compared with *siControl* treatment, with *siSUV39H1* acting by both accelerating fat accumulation in individual adipocytes and increasing the total number of committed adipocytes, whereas *siCITED2* acting predominantly by increasing the total number of committed adipocytes. In addition, both *siSUV39H1* and *siCITED2* were able to redirect hMSCs to undergo adipogenic differentiation in the presence of osteogenic inducing media, which normally only induces osteogenic differentiation of hMSCs in the absence of *siSUV39H1* or *siCITED2*. Interestingly, simultaneous knockdown of both SUV39H1 and CITED2 resulted in even greater levels of adipogenic differentiation of hMSCs and expression of CEBPα and PPARγ, two master regulators of adipogenesis, as compared with those elicited by single gene knockdown. Furthermore, the effects of co-knockdown were equivalent to the additive effect of individual gene knockdown. Taken together, this study demonstrates that SUV39H1 and CITED2 are both negative regulators of human adipogenesis, and downregulation of both genes exerts an additive effect on promoting adipogenic differentiation of hMSCs through augmented commitment.

Keywords: SUV39H1, CITED2, human mesenchymal stem cells (hMSCs), adipogenesis, additive effect and osteogenesis

Introduction

Obesity is characterized by excess body fat accumulation, as a result of increased number of adipocytes (fat cells) through adipogenesis and/or enlarged adipocytes due to increased lipid storage through lipogenesis [1]. Adipogenesis is the process in which uncommitted stem cells differentiate into mature adipocytes. Understanding the molecular and cellular regulation of human adipogenesis will help bring new insights on obesity and obesity-related diseases.

Much of our current understanding of adipogenesis is based on in vitro studies using mouse preadipocyte cell line 3T3L1 cells [2] and on a more limited scale, mesenchymal stem cells (MSCs) [3,4]. In both cell types, CEBPα (CCAAT/enhancer binding protein alpha) and PPARγ (peroxisome proliferator-activated receptor gamma) are two key players, whose deficiency in mice led to developmental defect in adipose tissue, and when overexpressed could dictate adipogenic cell fate in both 3T3L1 and hMSCs [5–9]. Human MSCs (hMSCs) are a type of adult stem cells that exist in multiple tissues, including adipose tissue, umbilical cord blood, Wharton's Jelly, and bone marrow, and play important roles in maintaining normal tissue homeostasis. Using adipogenic inducing media (AIM) containing a cocktail of dexamethasone (DEX) at 1 μM, 3-isobutyl-1-methylxanthine (IBMX) at 0.45 mM, and insulin at 10 μg/mL, hMSCs can be induced to differentiate into mature adipocytes, which makes them an excellent in vitro cellular model for studying human adipogenesis [10]. In addition to advancing our basic understanding of adipose tissue biology, hMSCs have been of great interest to researchers

Biological Sciences Department, California State Polytechnic University at Pomona, Pomona, California, USA.

exploring adipose tissue engineering and cell-based therapies due to their low allogeneic immune response and low tumorigenicity in graft recipients [11,12], which makes it even more relevant to use these cells for studying human adipogenesis.

In an effort to uncover negative regulators of human adipogenesis, a *siRNA*-based high-throughput screen was carried out to identify *siRNAs* that could promote hMSCs to undergo adipogenic differentiation, an approach that has been successfully used in the past to identify osteogenic suppressors of hMSCs [4]. Two identified *siRNA* targets, *siSUV39H1*, which targets Suppressor of variegation 3–9 homolog 1 (SUV39H1), and *siCITED2*, which targets a CBP/p300-interacting transactivator with Glu/Asp-rich carboxy-terminal domain 2 (CITED2), were chosen in this study for further investigation.

SUV39H1 is a H3K9 histone methyltransferase containing an N-terminal chromodomain and a C-terminal SET domain with catalytic activity [13–15]. A collection of evidence support that SUV39H1-mediated H3K9 methylation is closely associated with both chromatin silencing/inactivation and transcriptional repression. For example, SUV39H1 was shown to be recruited by Heterochromatin Protein 1 (HP1) through direct binding, which leads to increased level of H3K9me3, recruitment of additional proteins including DNA methyltransferase and subsequent formation of constitutive heterochromatin at pericentric and telomere region [16–19]. SUV39H1 was also shown to interact directly with both histone deacetylases (HDAC1/2) and retinoblastoma protein (Rb) to induce transcriptional repression on euchromatic gene promoters [20–22].

Histone methylation/demethylation activities have also been linked to the regulation of adipogenesis. Two types of histone methylation, H3K4 methylation and H3K9 methylation, appear to exert positive and repressive effect on adipogenic differentiation, respectively [23]. In 3T3-L1 cells, MLL3, a histone H3K4 methyltransferase, and PTIP, a PAX transactivation domain-interacting protein, have been shown to interact together to catalyze H3K4 trimethylation at the promoter regions of *CEBPα* and *PPARγ* and adipogenesis [24]. On the contrary, two other histone methyltransferase family members, SETDB1 and G9a, have been shown to promote H3K9 methylation immediately downstream of the transcription start site of *CEBPα* and across the entire *PPARγ* locus to form H3K9me3 and H3K9me2 domains, respectively, leading to subsequent repression of CEBPα and PPARγ expression and adipogenesis [25,26]. In both MSCs and 3T3-L1 cells, H3K4/H3K9me3 bivalent domains were found to keep developmental genes in a poised state for activation, and upon adipogenic stimulation the level of H3K4 methylation at the promoter regions of *CEBPα* and *PPARγ* was increased, while the level of H3K9 methylation was decreased, which coincided with the activation of these two genes and consequent adipogenic commitment [25,27].

However, few studies have examined the role of SUV39H1 in adipogenesis. Mice deficient in SUV39H1 alone exhibited no apparent phenotypes, but SUV39H1 and SUV39H2 double null mice displayed impaired viability and chromosome instability [16]. Overexpressing *SUV39H1* during early embryogenesis, on the contrary, led to growth retardation, weak penetrance of skeletal transformation, and impaired erythroid differentiation in mice [28], though it is not clear whether there was any perturbation of adipose tissue development. In 3T3-L1 preadipocytes, SUV39H1 was shown to methylate H3K9me2 to form H3K9me3, which repressed the expression of *CEBPα* along with AP-2α [29]. To our knowledge however, the role of SUV39H1 in human adipogenesis has not been examined in previous studies.

Similarly, the role of CITED2 in human adipogenesis has never been reported. CITED2 plays a critical role during embryonic development, as *CITED2* knockout mice were embryonically lethal due to defects in heart and neural tube formation [30]. It has been shown to act as a transcriptional modulator. For example, it served as a coactivator by physically and functionally interacting with AP-2 and p300/CBP to form a transcriptional complex [31]. It was also found to inhibit transactivation of hypoxia-inducible factor (HIF-1α)-induced genes by competitively blocking the interaction of HIF-1α with CBP/p300 [32]. The precise mode of action by CITED2 as a transcriptional modulator however is not clear.

While no studies have directly examined the role of CITED2 in adipogenesis, previous studies have implied that CITED2 may be involved in its regulation through its coregulators. For examples, both p300 and CBP are found to activate the expression of PPARγ and are indispensable for adipogenic differentiation [33]; in 3T3-L1 preadipocytes, AP-2α acts as a repressor of adipogenesis by repressing CEBPα expression [34]; and CITED2 is also an important modulator of transforming growth factor (TGF-β) signaling, which plays important role in adipogenesis [35,36]. Interestingly, both CBP and p300 are coactivators containing intrinsic HAT activity (H3K27) and can also recruit additional HATs to target genes' promoter regions [37]. CITED2 was also shown to interact with GCN5, also a HAT protein, in regulating the activity of PGC-1a and gluconeogenesis during fasting [38,39]. In addition, CITED2 interacted with HDAC1 to potentiate the MYC-HDAC1 complex formation to suppress downstream gene expression including $p21^{CIP1}$ [40]. It is therefore plausible that CITED2 may function as a transcriptional coregulator partly through histone acetylation modulation.

In this study, we report that both SUV39H1 and CITED2 are downregulated during normal adipogenic differentiation of hMSCs. Expression knockdown of SUV39H1 by siSUV39H1 significantly promoted adipogenic differentiation by both accelerating fat accumulation in individual adipocytes and enhancing adipogenic fate commitment of hMSCs, whereas siCITED2 elicited similar effect on enhancing adipogenic differentiation efficiency but mainly through enhancing adipogenic fate commitment of hMSCs. Double knockdown of both genes resulted in even greater enhancing effect that is equivalent to the cumulative effect of individual knockdown. The effect was at least partly mediated by the upregulation of CEBPα and PPARγ expression, as simultaneous knockdown of both SUV39H1 and CITED2 resulted in a cumulative increase in the expression of *CEBPα* and *PPARγ*, while downregulation of CEBPα diminished such effect. Taken together, our results demonstrated that SUV39H1 and CITED2 are both negative regulators of human adipogenesis, whose downregulation promotes the upregulation of CEBPα and PPARγ expression and subsequent adipogenic commitment in an additive manner.

Materials and Methods

hMSCs culture and differentiation

Adipose-tissue-derived hMSCs were purchased from Fisher Scientific (SV3010201) and cultured in Hyclone Advance STEM expansion media (CM) (Fisher Scientific, SH30875KT). Ad-hMSCs were expanded using 0.05% trypsin-EDTA (Corning; cat# 2502) and used at passage 4 (P4) for all assays. Human Dermal Fibroblasts (hDFs; ATCC, cat# PCS-201-012) were cultured in Hyclone Complete Media. Cells were grown in either Napco 8000wj CO_2 incubator TC/RH or Heracell CO_2 incubator with IR/RH and handled in Labconco biosafety cabinet.

For osteogenic differentiation induction, cells were exposed to an osteogenic inducing medium (OIM) composed of 0.05 mM ascorbic acid 2-phosphate (Sigma; 49752), 10 mM β-glycophosphate (Sigma; G9422), and 0.2 μM dexamethasone (Sigma; D4902) in CM. For adipogenic differentiation, adipogenic induction medium (AIM) was prepared in CM containing 0.45 mM 3-isobutyl-1-methylxanthine (IBMX; Sigma 15879), 10 μg/mL insulin (Sigma I9278-5ML), and 1 μM dexamethasone (DEX). Medium was changed every 48 h.

siRNA transfection

Reverse transfection, which was achieved by introducing *siRNA*-transfection reagent complex to culture vessel first followed by plating of cells, was conducted in all *siRNA* transfection experiments as previously described [4,41]. *SiRNA*-transfection reagent complex was prepared by diluting X-tremeGene *siRNA* transfection reagent (Sigma; cat# 04476093001) into a tube containing DMEM basal media (Thermofisher; cat #10566-16), followed by the addition of *siRNA* within 5 min. The complex was incubated for 25–30 min before cells were plated. Depending on experimental needs and cell culture vessel size, the ratio between the amount of *siRNA* and transfection reagent, and the number of cells transfected is proportionally adjusted (Supplementary Table S1).

The following *siRNAs* were used in this study: *siCON*: AllStars Neg. *siRNA* (Qiagen; cat#1027284); *siSUV39H1*/*siSUV39H1*-HTS (sequence: CCCGCAUGGACUCCAA CUU); *siSUV39H1–6* (Hs_SUV39H1_6, Qiagen; cat#-SI02665019); *siCITED2*-HTS (sequence: UGGGCGAG CACAUACACUA); *siCITED2–1* (Hs_CITED2_1, Qiagen; cat#SI00084252); *siCITED2–3* (Hs_CITED2_3, Qiagen; cat#SI00084266); *siCITED2–4* (Hs_CITED2_4, Qiagen; cat#SI00084273); *siCITED2/siCITED2–5* (Hs_CITED2_5, Qiagen; cat#SI03063102); *siCEBPα* (Hs_CEBPA_2, Qiagen; cat#SI00063189); and *siCDK1*: Hs_CDC2_9 (Qiagen; cat#I00299712).

Oil-Red-O and DAPI staining

Oil droplets in differentiated cells were stained by OilRedO solution (cat# NC9773107; Fisher Scientific). In brief, cells were fixed in 10% formalin for 20 min, rinsed with distilled water three times, washed in 100% isopropylene glycol for 5 min, incubated in Oil-Red-O solution for 30 min, washed with 85% isopropylene glycol for 5 min, and rinsed with distilled water three times. Cells were then counterstained with 1 μg/mL DAPI solution in PBS for 5 min before additional rinsing with water. Whole well images were taken with Leica EZD40 Stereoscope after staining. For OilRedO quantification, cells were air dried overnight in fume hood, extracted with pure isopropyl alcohol (cat# A426P; Fisher Scientific), transferred to a new 96-well plate, and OD was measured at 510 and 690 nm using a Biotek Elx800 plate reader.

Alizarin Red staining and quantification

Cells were washed one time with phosphate buffered saline (PBS) and then fixed for 15 min with 10% buffered formalin phosphate, followed by rinsing in distilled water three times. Fixed cells were incubated with 2% Alizarin Red S solution (pH 4.1–4.3, adjusted with 0.5% ammonium hydroxide, Acros Organic, cat#130-22-3) for 20 min, followed by four times washing with distilled water at 5-min intervals. Stained cells were air dried for imaging and quantification. Whole well images were taken by using a Leica dissection microscope. To quantify the calcium phosphate deposits, stained cells were incubated with 10% acetic acid for 30 min at room temperature. The loosely attached monolayer cells were scraped, and total well content was transferred to microcentrifuge tube. The mixtures were vortexed vigorously, followed by heating at 85°C for 10 min. The microcentrifuge tubes were then transferred to ice for 5 min until they were fully cooled. Next, the slurry was centrifuged at 20,000 *g* for 15 min, and the extracted supernatant dye solution was transferred to a new 96-well plate, and OD reading was measured at 405 and 690 nm using an ELx800 plate reader (BioTek).

Cell count analysis

To determine the total cell and mature adipocyte cell counts, cells stained by both DAPI and OilRedO were imaged using an Olympus IX50 microscope at 200× magnification (OilRedO: green light—red fluorescence; DAPI: UV light—blue fluorescence). For 96-well plate, images were taken from the bottom of the well to the top of the well on nonoverlapping area, capturing five separate fields of view per well. Total cell number was determined by counting DAPI-stained nuclei using CellProfiler software [42]. For mature adipocytes characterized by concentrated large oil droplets, they were manually counted based on merged DAPI and OilRedO images taken from the same field of view.

Gene expression by reverse transcription-PCR analysis

For cell sample collection, cells were detached with 0.05% trypsin-EDTA, washed once with 1× PBS, and stored at −80°C until RNA extraction. RNA was isolated from cells using the RNeasy kit (QIAGEN; cat#74134). The same amount of RNA was then reverse transcribed into cDNA using Superscript III Reverse Transcriptase Kit (Fisher Scientific; cat#11752). qPCR was carried out using the PowerUp SYBR Green Master Mix (Applied Biosystems; cat#A25780) and STEP ONE qPCR machine. Primers for *HSP90-beta* (control), *SUV39H1*, *CITED2*, *CEBPα*, *PPARγ*, *CDK1*, *FANCD2*, and *PLCB2* are listed in Supplementary Table S2. Quantifications are reported as average

expression for each gene of interest in treatment groups relative to that of control, after normalization to the expression level of internal control gene *HSP90*.

Western blot

Protein was extracted from whole cell lysis from 1.3×10^6 cells per treatment group using M-PER reagent (Thermofisher; cat#78501) containing 1×Halt protease inhibitor (Thermofisher; cat#87758). About 30 μg of protein per sample was loaded and separated in NuPAGE 10% bis-tris gel (Thermofisher; cat#NP0301BOX). After transferring to nitrocellulose membrane, the blot was incubated in antigen pretreatment solution (SuperSignal Western Blot Enhancer kit; Thermofisher, cat#46640) for 10 min before blocking the membrane using StaringBlock blocking buffer (Thermofisher; cat#37543), followed by incubation with primary antibody for one and half hour at room temperature, rinse in 1×TBS buffer for four times (5 min each), incubation with HRP-conjugated secondary antibody in blocking solution for 1 h at room temperature, and final rinse in TBS buffer for four times. Primary antibodies include the following: mouse monoclonal anti-HSP90 (Santa Cruz Biotechnology; cat# sc-13119); mouse monoclonal anti-beta-actin (Santa Cruz Biotechnology; cat# sc-47778); rabbit polyclonal anti-SUV39H1 (Abcam; ab155164); and rabbit monoclonal anti-CITED2—C-terminal (Abcam; ab108346). Secondary antibodies include goat antimouse IgG (Thermofisher; cat#31430) and goat antirabbit IgG (Abcam; ab6721).

Statistical analysis

Unpaired Student's *t*-test was used to evaluate the statistical differences between two sample groups, and both one-way ANOVA test and Student's *t*-test were used to evaluate the statistical differences among multiple sample groups.

Results

siRNA-*based high-throughput screen identifies suppressors of human adipogenesis*

In an effort to uncover suppressors of human adipogenesis, a *siRNA*-based high-throughput screen was carried out (Zhao, PNAS, 2007), in which *siRNAs* against 5,000 genes were introduced into hMSCs, followed by media treatment containing DEX (0.1 μM). DEX is a synthetic glucocorticoid agonist that acts as a stimulating agent during differentiation of MSCs, with high concentration of DEX promoting adipogenesis while inhibiting osteogenesis [43,44]. By itself, it is insufficient to induce mature adipocyte formation even at a high concentration (1 μM). In consideration of the slim possibility that any individual *siRNA* alone would induce hMSCs to fully undergo adipogenesis, low concentration of DEX at 0.1 μM was used as a sensitizer in the screen by treating cells with DEX containing growth media for 21 days post-*siRNA* transfection. By comparing with *siControl*, a group of scrambled *siRNAs* that do not target any genes in the human genome, *siRNAs* that could induce hMSCs to give rise to distinctively greater number of adipocytes in the presence of 0.1 μM DEX were identified (Supplementary Fig. S1). Among the *siRNA* hits identified, *siSUV39H1*-HTS, which targets SUV39H1, a histone methyltransferase that catalyzes H3K9Me3, consistently gave rise to the strongest phenotype based on abundance of mature adipocytes in two independent screens of the same *siRNA* library. Of the remaining hits, *siCITED2*-HTS was also chosen for further investigation due to its modestly strong phenotype and the potential role of CITED2 in regulating histone acetylation [37–40].

Expression knockdown of SUV39H1 *and* CITED2 *enhanced adipogenic differentiation of hMSCs independent of media type*

To further confirm the effect of *siSUV39H1* and *siCITED2* on adipogenic differentiation of hMSCs observed in the high-throughput screen, additional *siRNA* sequences (*siSUV39H1–6*, *siCITED2–1*, *siCITED2–3*, *siCITED2–4,* and *siCITED2–5*) targeting each of the genes were selected and further tested based on their commercial status of ''functionally validated.'' Each *siRNA* sequence was individually examined by transfecting into hMSCs (at ~95% confluent density) in growth media (CM) at 18.5 nM for 24 h, followed by AIM treatment (Materials and Methods section) and subsequent media change at 48-h intervals. For each experimental set, there were six wells per treatment group, and groups on the same 96-well plate were symmetrically positioned to avoid any potential positional effect on the differentiation outcome. Great care was also taken to ensure that equal amounts of hMSCs were plated across all treatment wells during transfection. After 14 or 21 days of AIM treatment post-transfection, cells were then fixed, stained with OilRedO solution, imaged and quantified, with the amount of extracted OilRedO dye reflecting the total amount of fat in the form of oil droplets formed inside cells. For *siSUV39H1–6* against SUV39H1, it did not elicit the same adipogenic effect as demonstrated by the *siSUV39H1*-HTS sequence identified from the *siRNA* library (Supplementary Fig. S2a). Of the four different *siRNA*s against CITED2 that were tested however, *siCITED2–5* demonstrated an adipogenic enhancement effect similar to what was observed from the *siCITED2*-HTS sequence identified from the *siRNA* library (Supplementary Fig. S2b and data not shown). Both *siSUV39H1*-HTS and *siCITED2*–5 were subsequently used for the remainder of this study and for simplicity, designated as *siSUV39H1* and *siCITED2,* respectively.

The effect of *siSUV39H1* and *siCITED2* on adipogenic differentiation of hMSCs was further verified in at least three independent biological replicates, demonstrated by greater OilRedO stain intensity as shown in whole well images and an increase in OilRedO stain quantification by 1.63-fold and 1.35-fold, respectively, relative to their *siControl* group at day 14 post-AIM initiation (Fig. 1). Since the Hyclone growth media (CM) used in composing the AIM for adipogenic induction is a proprietary product, to eliminate the possibility that the observed adipogenic enhancement effect was Hyclone CM dependent, the effect of *siSUV39H1* was also examined using AIM based on standard cell culture media containing 90% high-glucose DMEM and 10% FBS. Similar to previous experiments, hMSCs were transfected with either *siSUV39H1* or *siControl* for 24 h, followed by 14 days of AIM treatment based on (DMEM+FBS) or Hyclone CM (as parallel control). Cells were subsequently stained and quantified. Again, regardless

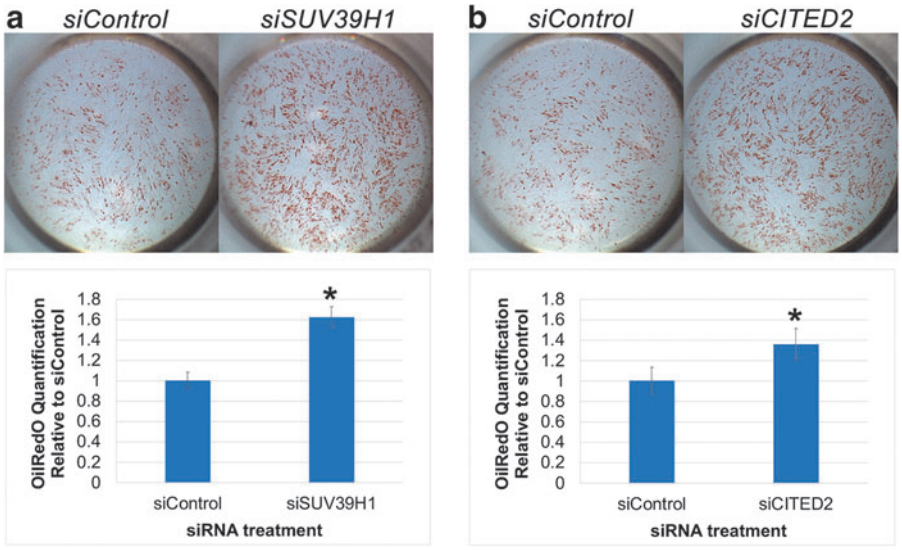

FIG. 1. **(a, b)** *siSUV39H1* and *siCITED2* enhanced adipogenic differentiation of hMSCs. *Top panels*: representative whole well images were taken after 14-day AIM treatment post-*siRNA* transfection; *bottom panels*: OilRedO quantification relative to *siControl* treatment group. Data represent the average of four (SUV39H1) or three (CITED2) independent experimental replicates with six wells per treatment group per experimental set. $*P < 0.01$.

of the media type, there was significant increase in the total amount of oil droplets formed in the *siSUV39H1* treatment group compared with the *siControl* group, as demonstrated by both phenotypic visualization and OilRedO dye quantification (Supplementary Fig. S3). The results above further confirmed that knockdown of *SUV39H1* and *CITED2* indeed significantly enhanced adipogenic differentiation of hMSCs, and such effect was independent of the growth media type used to constitute the AIM.

Temporal expression patterns of SUV39H1 *and* CITED2 *during adipogenic differentiation of HMSCs*

To examine the expression patterns of *SUV39H1* and *CITED2* during normal adipogenic differentiation of hMSCs, cells were plated at ~95% confluent density on Day (-1), and RT-PCR was carried out on cell samples isolated at 24 (Day 1), 48 (Day 2), 72 (Day 3), 96 (Day 4), 120 (Day 5), and 144 (Day 6) hours post-AIM induction (Day 0), with media change at every 48 h (samples were collected without media change on even days). Cell samples treated in parallel with growth media (CM) at each time point were used for comparison, with Day 1 samples serving as real-time PCR reference control. To verify primer pair specificity against each gene, PCR products were run on agarose gel for DNA band isolation and subsequent sequencing to make sure that the amplified products indeed matched to the sequence of its targeted gene (data not shown). In CM treatment groups, expression of both *SUV39H1* and *CITED2* appeared to oscillate in response to media change, with higher expression on odd days as compared with even days (Fig. 2a, b). On the contrary, their expression was significantly reduced at 24 h post-AIM initiation as compared with their expression level at the same time point in the CM reference control sample ($P < 0.01$), and remained at a steadily low level afterward (Fig. 2a, b). The results indicated that both SUV39H1 and CITED2 were significantly downregulated within the first 24 h of adipogenic induction and remained at a low level of expression afterward.

Expression knockdown of SUV39H1 *and* CITED2 *correlates to enhanced adipogenic differentiation induced by* siSUV39H1 *and* siCITED2, *respectively*

To confirm that *siSUV39H1* and *siCITED2* did indeed downregulate the expression of SUV39H1 and CITED2, respectively, both RT-PCR and Western blot were carried out to examine the expression of these genes in hMSCs post-*siSUV39H1* or *siCITED2* transfection in comparison with their expression in cells transfected with *siControl*. After 24 h of *siRNA* transfection, cells were treated with AIM followed by media change at 48-h intervals, and samples were isolated at day 1, 2, 3, 4, or 5 post-*siRNA* transfection (samples were collected without media change on even days). Expression of each gene in *siSUV39H1*- or *siCITED2*-treated cells was quantified relative to its expression in *siControl*-treated cells after normalization against the expression of internal control gene *HSP90* at each time point. RT-PCR results indicated that expression of SUV39H1 in *siSUV39H1* samples was reduced to 25%–45% of its level in *siControl* samples starting from 24 h post-transfection (Day 1) and lasted until at least Day 5 (Fig. 3a). Expression of CITED2 was only slightly knocked down within 48 h of *siCITED2* treatment, but further reduced to 30%–50% of its control level afterward (Fig. 3b). At the protein level however, expression knockdown appeared to be more modest relative to that at the *RNA* level, with expression of SUV39H1 in *siSUV39H1* reduced to 45%–75% of its expression level in *siControl* and expression of CITED2 in *siCITED2* reduced to 64%–75% of its expression level in *siControl* on Day 3 and Day 5 post-transfection (Fig. 3).

Since two different *siRNA* sequences against CITED2, *siCITED2*-HTS and *siCITED2/siCITED2–5*, were identified to demonstrate similar adipogenic enhancement effect, whereas only one *siRNA* sequence against *SUV39H1*, *siSUV39H1/*siSUV39H1-HTS, was identified to elicit such effect, the 19-bp sequence of *siSUV39H1* was blasted against the whole genome to identify additional potential targets, in an effort to further verify target specificity of *siSUV39H1* against SUV39H1. Only two genes with significant sequence match, FANCD2 (15 bps match) and

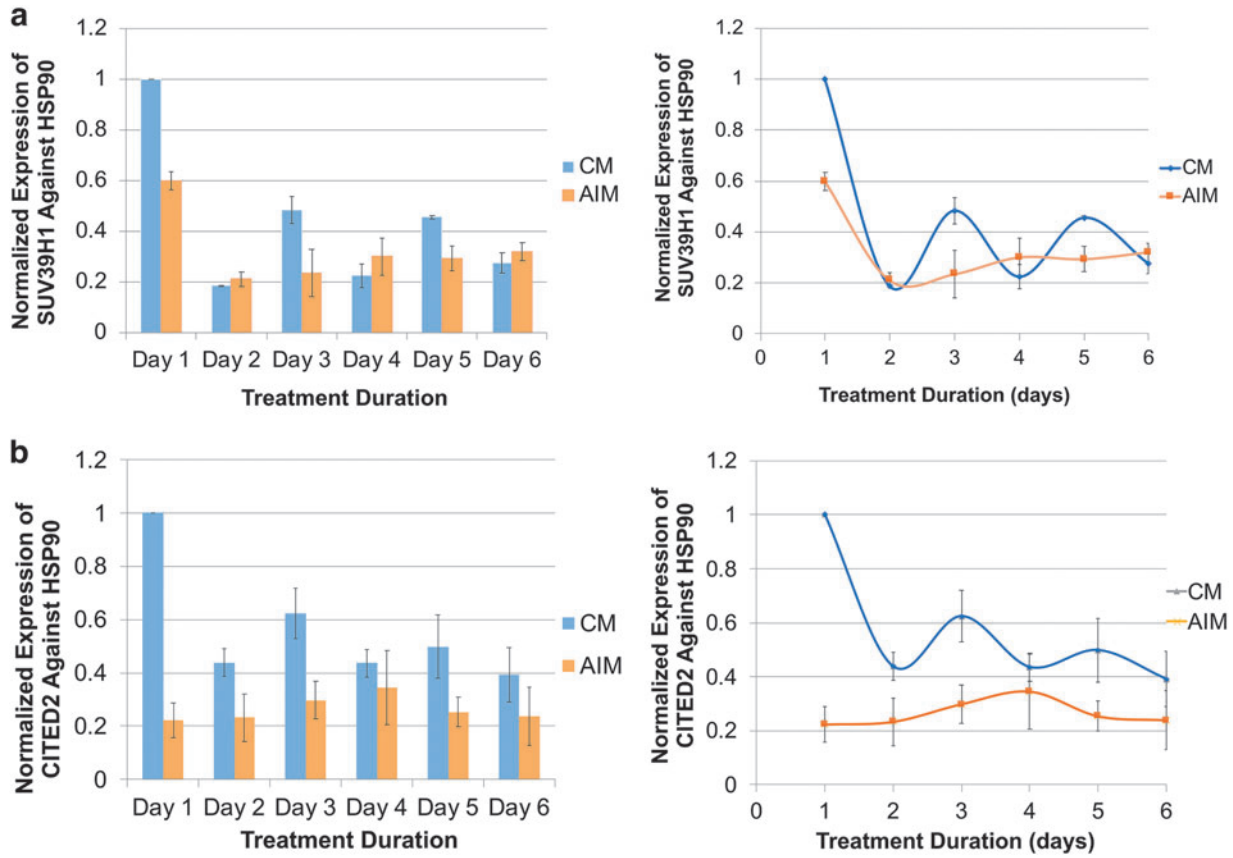

FIG. 2. Expression of SUV39H1 and CITED2 was downregulated during normal adipogenic differentiation of hMSCs. Expression of SUV39H1 **(a)** and CITED2 **(b)** was normalized against that of internal control gene HSP90, and graphed relative to its expression level in CM-treated sample on Day 1. CM, complete growth media; AIM, adipogenic inducing media. Data were derived from the average of three (SUV39H1) or four (CITED2) technical replicates from one experimental set.

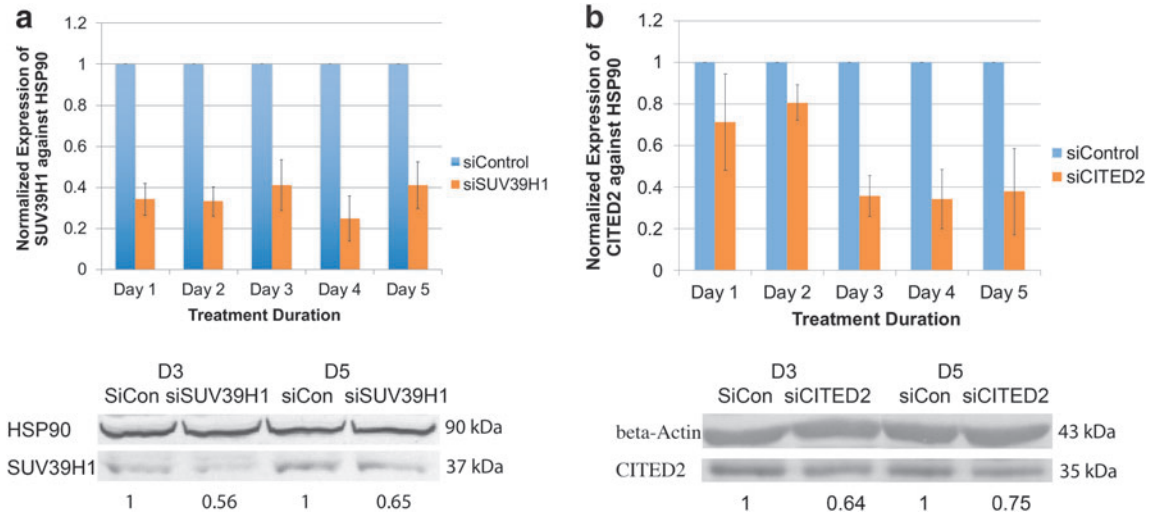

FIG. 3. Expression of SUV39H1 and CITED2 was downregulated by *siSUV39H1* and *siCITED2,* respectively. Expression of SUV39H1 **(a)** and CITED2 **(b)** at both RNA (*top panels*) and protein levels (*bottom panels*) was detected by RT-PCR and Western blot, respectively, at day 1, 2, 3, 4, and 5 post-*siRNA* transfection. RT-PCR data for days 1, 2, and 4 were derived from the average of three technical replicates from one experimental set, and data for days 3 and 5 were derived from the average of three independent experimental replicates. Western blot data were taken from one experimental set representative of three independent experimental replicates.

PLCB2 (14 bps match), were identified. To examine whether these genes were downregulated by *siSUV39H1*, RT-PCR was performed on these genes in *siSUV39H1*- and *siControl*-transfected cells. In both cases, expression was not downregulated in response to *siSUV39H1* (data not shown). In addition, expression of SUV39H1 was examined in cell samples transfected with *siSUV39H1–6*, which did not elicit a phenotypic effect, and compared with its expression in *siControl,* and again no downregulation was observed at either the mRNA or protein level (data not shown).

Taken together, the above results demonstrated that expression knockdown of SUV39H1 and CITED2 at both the *mRNA* and protein levels correlated with the adipogenic enhancement effect induced by *siSUV39H1* and *siCITED2*, respectively.

siSUV39H1 *and* siCITED2 *enhanced adipogenic differentiation of HMSCs through accelerated and/or augmented adipogenic commitment*

Increased total fat accumulation could be the result of increased adipocyte numbers (hyperplasia) and/or increased fat accumulation within individual adipocytes (hypertrophy). To help assess the underlying cause(s), total cell numbers and adipocyte cell counts were counted and compared between *siSUV39H1/siCITED2* and *siControl* groups using images taken from DAPI (stains nuclei) and OilRedO double-stained cells at the end of 14-day AIM treatment, and the percentage of adipocytes (adipocytes%) calculated by (adipocyte number/total cell number) was subsequently determined. In both cases, while total cell numbers in the siSUV39H1 or siCITED2 group in general trended lower than those of the *siControl* group, total adipocytes in *siSUV39H1* and *siCITED2* had $\sim$2.4-fold and 1.4-fold increase, respectively, than those in *siControl* (data not shown). As a result, the percentage of adipocytes was also significantly higher in *siSUV39H1* and *siCITED2* than in *siControl* by $\sim$2.4-fold and 1.4-fold, respectively (Fig. 4 and additional data not shown). The results clearly indicated that both *siSUV39H1* and *siCITED2* enhanced adipogenic differentiation of hMSCs by increasing the total number of adipocytes without significantly affecting total cell numbers (hyperplasia) during a 14-day differentiation period.

Increased number of adipocytes observed in *siSUV39H1* and *siCITED2* could be due to accelerated adipogenic commitment and accumulation of oil droplets in individual adipocytes, making them more identifiable by day 14, and/or due to augmented potential of individual hMSCs to become adipocytes. The former was partly supported by visual observation that individual adipocytes were recognizable at an earlier time point post-AIM initiation in *siSUV39H1/siCITED2*-treated wells as compared with *siControl* wells (data not shown). To examine these two possibilities, cells transfected with *siSUV39H1/siCITED2* or *siControl* were treated with AIM for 14 days (D14), 21 days (D21), 30 days (D30), or 60 days (D60), and differentiation outcomes were compared between treatment groups at each time point and across different time points within each group.

Across all time points, *siSUV39H1*-treated wells showed stronger OilRedO staining intensity as compared with *siControl* wells (Fig. 4a). OilRedO quantification further confirmed statistically significantly greater fat accumulation in *siSUV39H1* group than in *siControl* group at all time points (Fig. 4b), with 1.73-fold, 1.40-fold, 1.21-fold, and 1.25-fold increase at Days 14, 21, 30, and 60, respectively. Total cell numbers trended lower in *siSUV39H1* treatment groups as compared with *siControl* controls, though the difference was not statistically significant (Fig. 4c). On the contrary, *siSUV39H1* treatment groups consistently had greater number of adipocytes across all time points (data not shown), and consequently, greater percentage of adipocytes as compared with *siControl* at all time points as well, with 2.44-fold, 1.89-fold, 1.50-fold, and 1.76-fold increase at Days 14, 21, 30, and 60, respectively, all statistically significant increases (Fig. 4d). Interestingly, while the percentage of adipocytes in *siControl* significantly increased over time and stabilized at Days 30 and 60, the percentage of adipocytes in *siSUV39H1* appeared relatively unchanged across all time points (Fig. 4d). The results indicated that overall adipocyte commitment in *siControl* did not plateau until around day 30 post-AIM initiation, whereas that of *siSUV39H1* reached saturation by day 14 already, at a much faster pace than the *siControl* group. Nevertheless, regardless of short-term or long-term culture, *siSUV39H1* treatment group always had significantly greater number of adipocytes as compared with *siControl*, indicating that *siSUV39H1* also significantly augmented the number of hMSCs capable of committing to adipogenic lineage. Taken together, the results demonstrated that increased adipogenic differentiation efficiency induced by *siSUV39H1* was due to both accelerated adipogenic commitment and fat accumulation in some cells normally capable of committing to adipogenic cell fate, as well as augmented adipogenic commitment by potentiating individual hMSCs that normally do not respond to AIM to undergo differentiation.

Similarly, when comparing *siCITED2* vs. *siControl* treatment groups, OilRedO staining intensity in *siCITED2* wells was visually stronger than that in *siControl* wells across all time points (Fig. 4a). OilRedO quantification confirmed statistically significantly greater amount of fat accumulation in *siCITED2* group than in *siControl* group at all time points as well, with 1.30-fold, 1.21-fold, 1.22-fold, and 1.31-fold increase at Days 14, 21, 30, and 60, respectively (Fig. 4b). Total cell numbers were in par or trended lower in *siCITED2* treatment group when compared with *siControl* group (Fig. 4c), but the *siCITED2* treatment group consistently had greater number of adipocytes and consequently, significantly greater percentage of adipocytes as compared with *siControl* at all time points as well, with 1.38-fold, 1.32-fold, 1.25-fold, and 1.21-fold increase at Days 14, 21, 30, and 60, respectively (Fig. 4d). However, unlike the *siSUV39H1* treatment group, the percentage of adipocytes in *siCITED2* treatment group gradually increased over time at a similar rate as seen in the *siControl* group, which plateaued at Day 30 (Fig. 4d), indicating that *siCITED2* promoted adipogenic differentiation of hMSCs not likely by accelerating adipogenic commitment and maturation, but rather through augmented adipogenic commitment by potentiating individual hMSCs that normally do not respond to AIM to undergo differentiation.

Finally, to examine whether hypertrophy, an increase in adipocyte cell size, could also be a contributing factor to the increased total fat accumulation induced by *siSUV39H1* and *siCITED2*, stained oil droplets in individual adipocytes

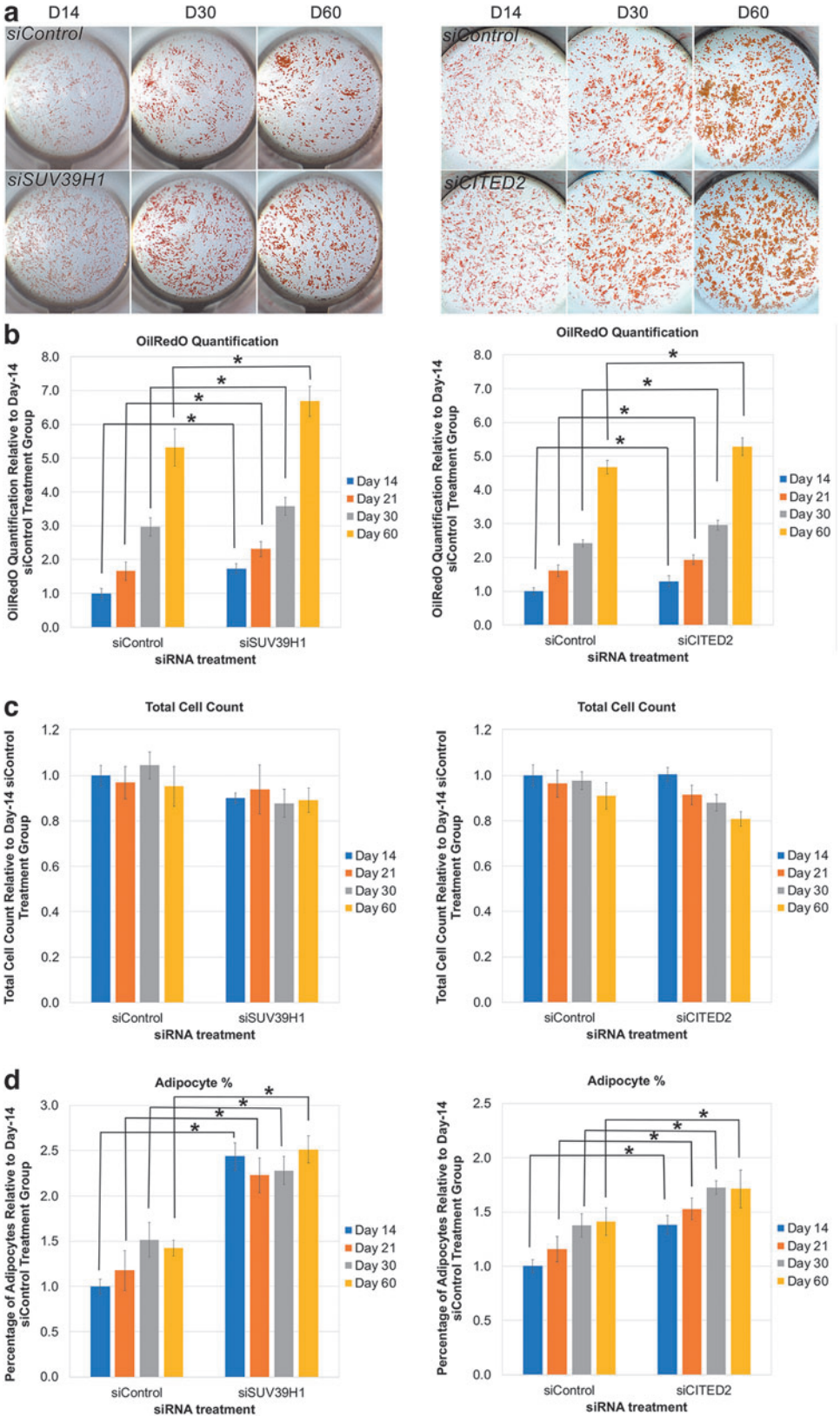

FIG. 4. *siSUV39H1* and *siCITED2* accelerated and/or augmented adipogenic commitment of hMSC revealed through long-term versus short-term differentiation comparison. In each experimental set, *siRNA*-transfected cells were treated with AIM for 14, 21, 30, or 60 days before fixation and staining, with six wells per *siRNA* treatment group at each time point. **(a)** Representative whole well images of cells stained with OilRedO solution after 14, 30, or 60 days of AIM treatment; **(b)** OilRedO quantification relative to the level in Day 14 *siControl* treatment group; **(c)** total cells quantification relative to cell count in Day 14 *siControl* treatment group; **(d)** percentage of adipocytes quantification relative to the level in Day 14 *siControl* treatment group. Quantification data for **(b–d)** were derived from the average of two (*siSUV39H1* vs. *siControl*) or three (*siCITED2* vs. *siControl*) independent experimental replicates. $*P < 0.01$.

were measured and compared between treatment groups, *siSUV39H1* versus *siControl* and *siCITED2* versus *siControl*, after 14 or 60 days of adipogenic induction by using ImageJ Nuclear Morphometric Analysis software [45]. Interestingly, at Day 14, the size of adipocytes in both *siSUV39H1* and *siCITED2* treatment groups was smaller than that in the *siControl* control group, with P values of 0.0117 and 0.0685, respectively (Supplementary Fig. S4). By Day 60 however, there was no significant difference between any of the treatment groups (Supplementary Fig. S4). The results

above demonstrated that during short-term differentiation (14 days), at least some of the cells in the *siSUV39H1* and *siCITED2* treatment groups had less fat accumulation than those in the *siControl* control group, but by day 60, the average cell size of mature adipocytes in all treatment groups was about the same. Taken together, the results indicate that regardless of the duration of AIM treatment, hypertrophy was not a contributing factor to the increased total fat accumulation induced by *siSUV39H1* and *siCITED2*.

siSUV39H1 *and* siCITED2 *both inhibited osteogenic differentiation of HMSCs while promoting adipogenic differentiation in osteogenic induction condition*

Since adipogenic and osteogenic differentiation are known to be two inversed processes, with one inhibiting the other [4,46], the role of SUV39H1 and CITED2 in osteogenic differentiation was also investigated. HMSCs were reverse transfected with *siSUV39H1, siCITED2,* or *siControl* followed by 21 days of OIM treatment, with media change at 48-h intervals. Cells were then fixed and stained with either Alizarin Red S, which specifically stains for calcium phosphate deposits secreted by osteocytes, or OilRedO for the presence of adipocytes in replicate sets of wells. Alizarin Red S dye was subsequently extracted with acetic acid and quantified by optical density reading at 405 nm. Whole well images clearly showed much lower intensity of Alizarin Red S stains in *siSUV39H1* and *siCITED2* wells as compared with *siControl* wells (Fig. 5a), and consistently, Alizarin Red S quantification was statistically significantly lower in *siSUV39H1*-treated samples (43%, $P<0.01$) and *siCITED2* samples (22%, $P<0.01$) as compared with *siControl* samples (100%) (Fig. 5a). On the contrary, while few adipocytes were found in *siControl* wells, adipocytes were abundantly present in both *siSUV39H1* and *siCITED2* wells, with especially greater amounts in the *siSUV39H1* treatment wells (Fig. 5b). Overall, the above results demonstrated that expression knockdown of SUV39H1 and CITED2 strongly inhibited osteogenic differentiation but promoted adipogenic differentiation of hMSCs under osteogenic induction condition.

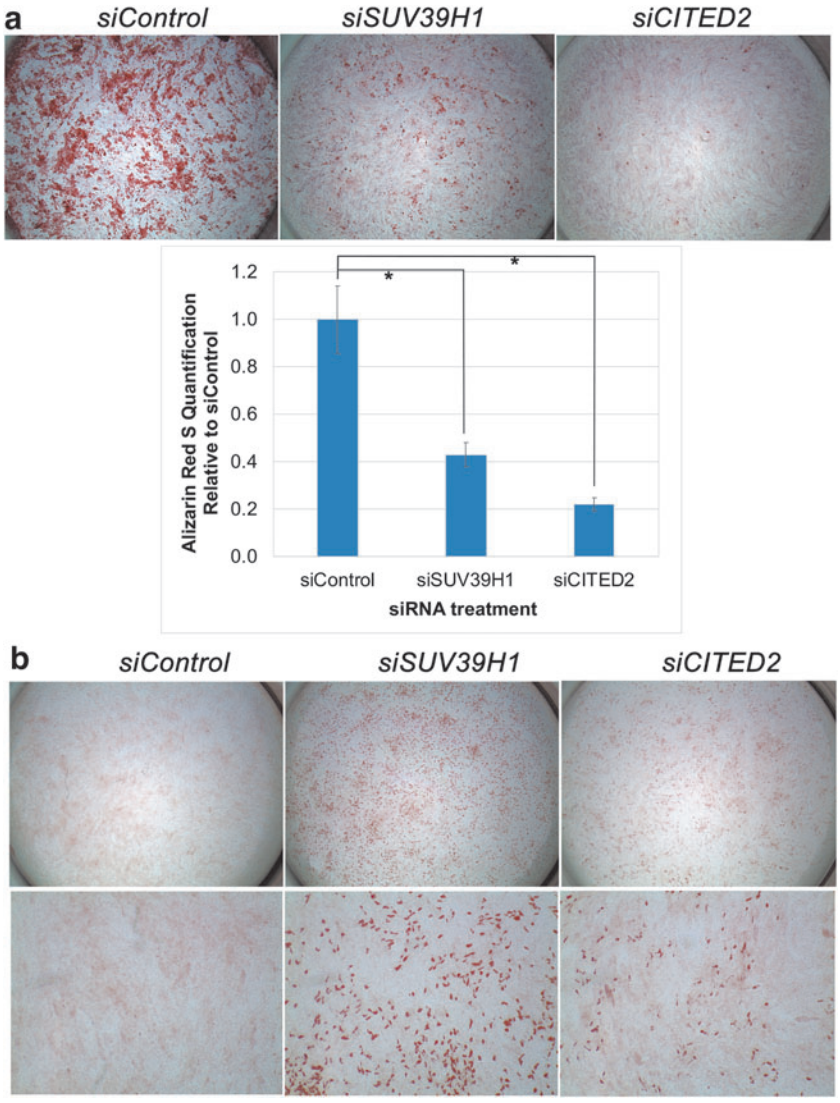

FIG. 5. *siSUV39H1* and *siCITED2* inhibited osteogenic differentiation of hMSCs while promoting adipogenic differentiation under osteogenic induction condition. In this experiment, *siControl*-, *siSUV39H1*-, and *siCITED2*-treated cells were compared in parallel in each experimental set, with 12 wells per treatment group of which half were stained with Alizarin *Red* S and the other half stained with OilRedO after 21 days of OIM treatment post-*siRNA* transfection. **(a)** Representative whole well images of cells stained with Alizarin *Red* S and Alizarin *Red* S stain quantification; **(b)** representative whole well images of cells stained with OilRedO solution (*top row*) and images magnified by 35× (*bottom row*). Images and quantification data were derived from a representative experimental set of three independent experimental replicates showing similar results. *$P<0.01$.

siSUV39H1 *and* siCITED2 *co-knockdown exerted additive effect on promoting adipogenic differentiation of HMSCs*

Since expression knockdown of either SUV39H1 or CITED2 promoted adipogenic differentiation of hMSCs through augmented adipogenic commitment, the effect of knocking down both was further investigated by transfecting cells with (*siControl* + *siControl*), (*siControl* + *siCITED2*), (*siControl* + *siSUV39H1*), or (*siCITED2* + *siSUV39H1*) (see materials and methods). After 24 h of transfection, adipogenic differentiation was initiated by AIM, with media change at 48-h intervals. Cells were subsequently fixed at day 14 or day 30, stained and analyzed as previously described.

As expected, both (*siControl* + *siCITED2*) and (*siControl* + *siSUV39H1*) groups showed stronger intensity of OilRedO stain as compared with (*siControl* + *siControl*) group at both day 14 (one biological replicate, data not shown) and day 30 (two biological replicates, Fig. 6a), which was further confirmed by OilRedO quantification (Fig. 6b). Interestingly, at both time points, (*siCITED2* + *siSUV39H1*) also consistently demonstrated statistically significantly stronger OilRedO stain than both (*siControl* + *siCITED2*) and (*siControl* + *siSUV39H1*) treatment group (Fig. 6a, b). Total cell numbers in (*siCITED2* + *siSUV39H1*) were not statistically significantly different from those in (*siControl* + *siCITED2*) or (*siControl* + *siSUV39H1*) groups (data not shown), but the percentage of adipocytes was significantly higher in the former (Fig. 6c). Intriguingly, the percentage of adipocytes

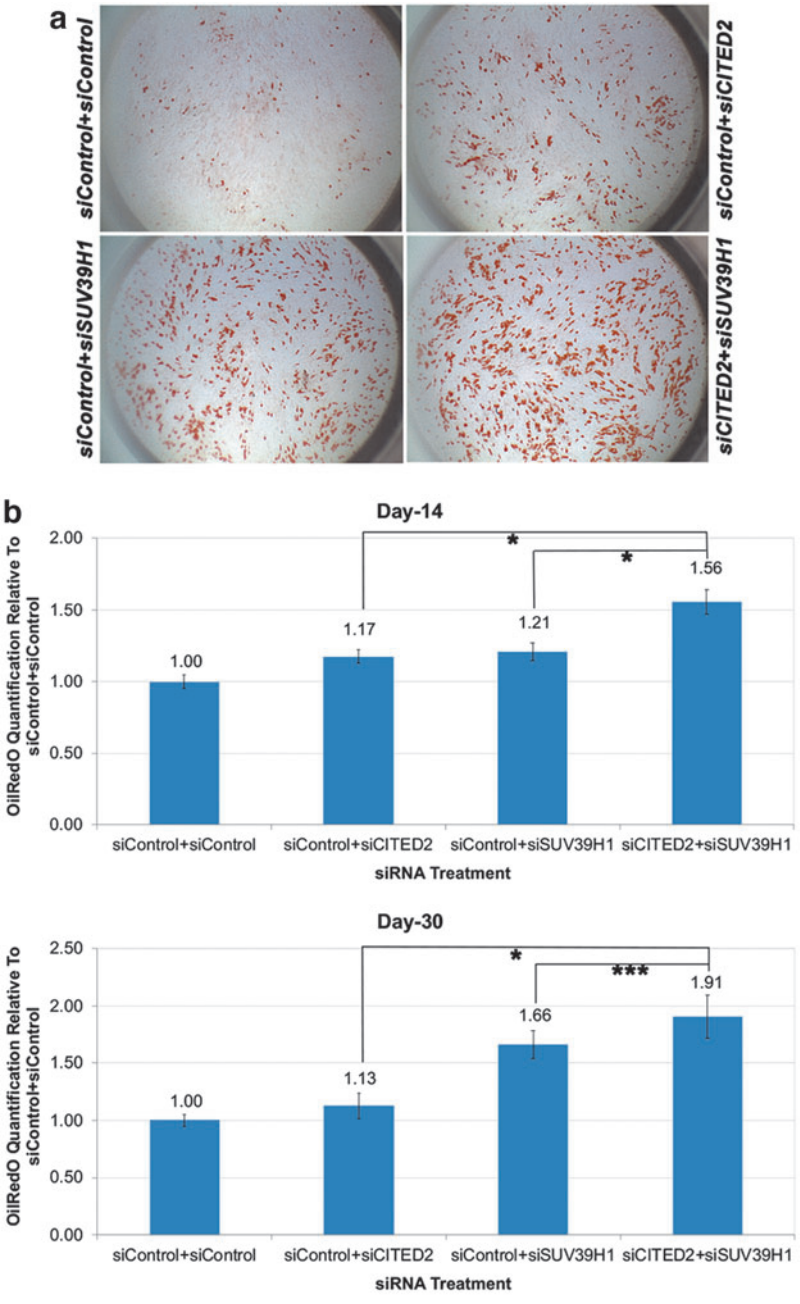

FIG. 6. *siSUV39H1* and *siCITED2* co-knockdown exerted cumulative effect on promoting adipogenic differentiation of hMSCs. Cells transfected with (*siControl* + *siControl*), (*siControl* + *siCITED2*), (*siControl* + *siSUV39H1*), or (*siCITED2* + *siSUV39H1*) were treated with AIM for 14 (one experimental set) or 30 days (two independent experimental replicates) before fixation, staining, and quantification, with six wells per treatment group in each experimental set. **(a)** Representative whole well images of cells stained with OilRedO after 30-day treatment; **(b)** OilRedO quantification relative to the level in (*siControl* + *siControl*) control at 14 (*top panel*) or 30 days (*bottom panel*) post-AIM initiation. **(c)** Percentage of adipocytes quantification relative to the level in (*siControl* + *siControl*) control at 14 (*top panel*) or 30 days (*bottom panel*) post-AIM initiation. $*P < 0.01$; $**P < 0.05$; $***P < 0.1$.

(*continued*)

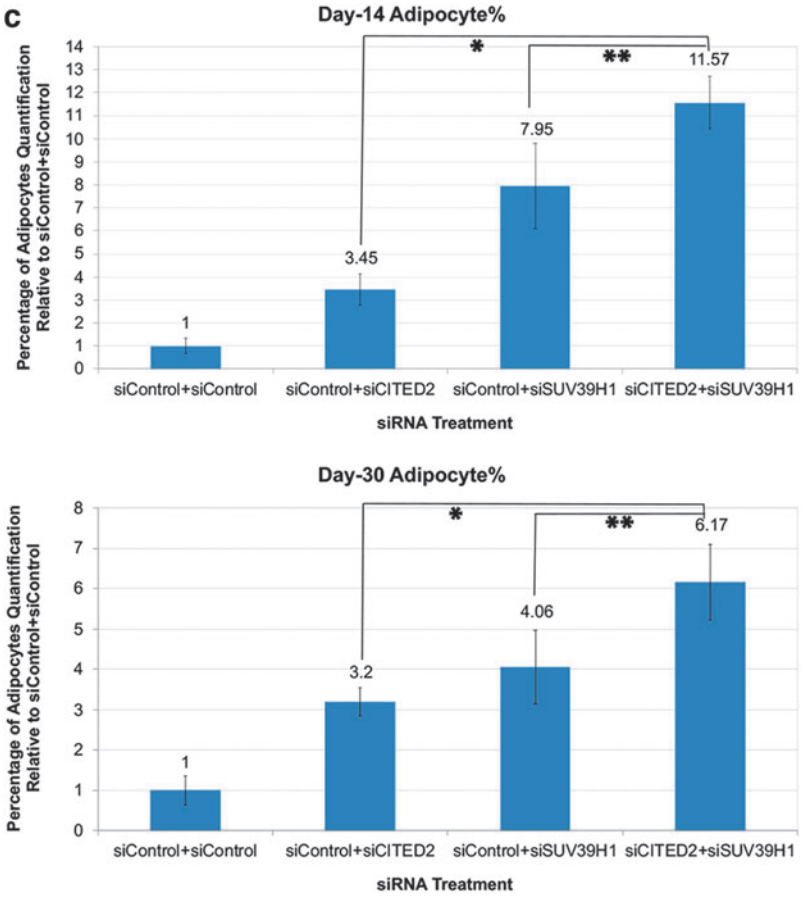

FIG. 6. (Continued).

in (*siCITED2* + *siSUV39H1*) was increased by 10.6-fold over (*siControl* + *siControl*) at day 14, which is approximately the sum of fold increases induced by (*siControl* + *siCITED2*) (2.5-fold) and (*siControl* + *siSUV39H1*) (7.0-fold) (Fig. 6c). Similarly, at day 30, the percentage of adipocytes in (*siCITED2* + *siSUV39H1*) was increased by 5.2-fold over (*siControl* + *siControl*), which is very close to the sum of fold increase induced by (*siControl* + *siCITED2*) (2.2-fold) and (*siControl* + *siSUV39H1*) (3.1-fold) (Fig. 6c). The results above indicate that the effect of CITED2 and SUV39H1 co-knockdown on the adipogenic differentiation efficiency of hMSCs was approximate to the additive effect of individual gene knockdown.

SUV39H1 *and* CITED2 *co-knockdown exerted additive effect on promoting the expression of* CEBPα *and* PPARγ

CEBPα and *PPARγ* are two master regulators of adipogenesis, which when overexpressed could dictate adipogenic cell fate in both murine 3T3L1 cells and hMSCs [5–9]. Our previous study found that they were highly upregulated during the commitment stage (Days 3–6) of adipogenic differentiation of hMSCs induced by AIM [41]. To examine whether the effect of *siCITED2* and *siSUV39H1* on adipogenic differentiation was mediated by regulating the expression of *CEBPα* and *PPARγ*, RT-qPCR was performed on (*siControl* + *siControl*), (*siControl* + *siCITED2*), (*siControl* + *siSUV39H1*), and (*siCITED2* + *siSUV39H1*) treated samples at day 3, 5, and 7 postadipogenic initiation. Expression changes in *CEBPα* and *PPARγ* in response to *siCITED2* and/or *siSUV39H1* were measured by comparing their expression levels in (*siControl* + *siCITED2*), (*siControl* + *siSUV39H1*), and (*siCITED2* + *siSUV39H1*) with that in (*siControl* + *siControl*) at the same time point, after normalization against the expression level of internal control gene *HSP90*.

Expression of both *CEBPα* and *PPARγ* was higher in (*siControl* + *siCITED2*), (*siControl* + *siSUV39H1*), and (*siCITED2* + *siSUV39H1*) compared with (*siControl* + *siControl*) at all time points (Fig. 7). Furthermore, their fold increase in (*siCITED2* + *siSUV39H1*) was approximate to the sum of fold increases in (*siControl* + *siCITED2*) and (*siControl* + *siSUV39H1*): at Day 3, expression fold change of *CEBPα* and *PPARγ* in (*siCITED2* + *siSUV39H1*) over (*siControl* + *siControl*) was 9.60-fold and 3.25-fold, respectively, which were approximate to the sum of their fold increases in (*siControl* + *siCITED2*) and (*siControl* + *siSUV39H1*), at 1.56-fold and 7.31-fold, respectively, for *CEBPα*, and 0.75-fold and 2.08-fold, respectively, for *PPARγ*; at Day 5, expression fold change of *CEBPα* and *PPARγ* in (*siCITED2* + *siSUV39H1*) over (*siControl* + *siControl*) was 8.83-fold and 3.41-fold, respectively, which were approximate to the sum of their fold increases in (*siControl* + *siCITED2*) and (*siControl* + *siSUV39H1*), at 3.77-fold and 6.35-fold, respectively, for *CEBPα*, and 1.37-fold and 2.25-fold, respectively, for *PPARγ*; at Day 7, expression fold change of *CEBPα* and *PPARγ* in (*siCITED2* + *siSUV39H1*) over (*siControl* + *siControl*) was 17.43-fold and 5.63-fold,

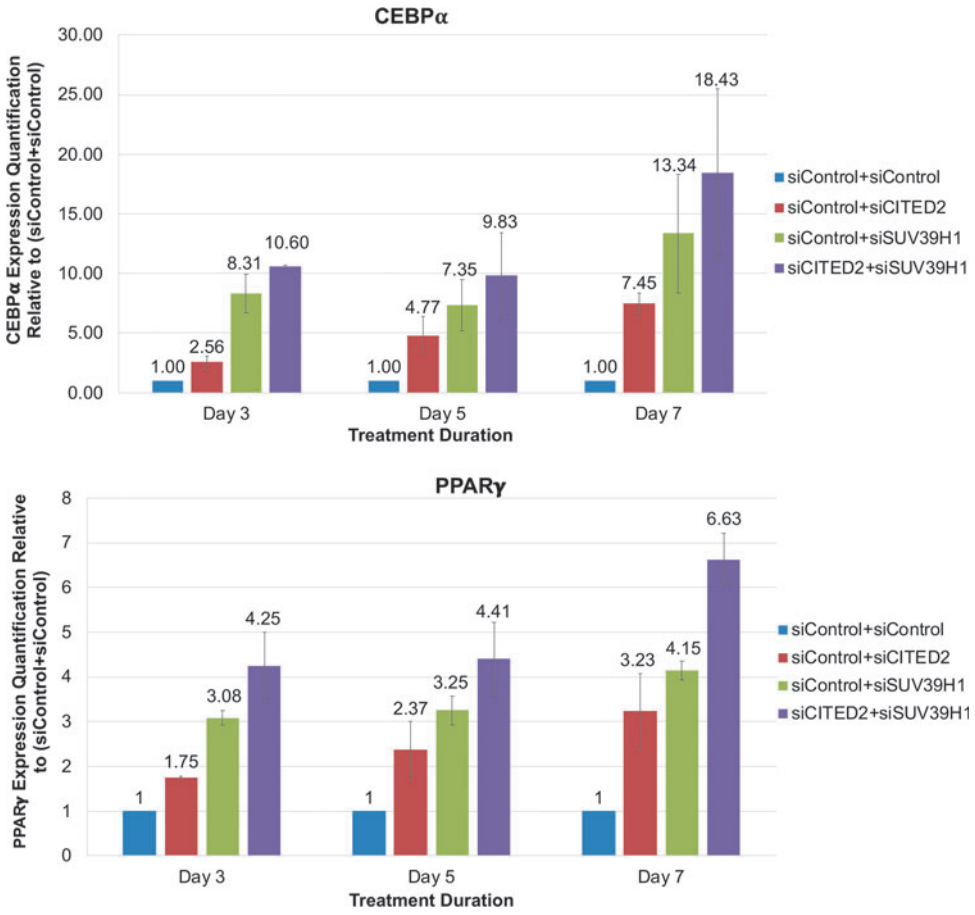

FIG. 7. *siSUV39H1* and *siCITED2* co-knockdown exerted cumulative effect on enhancing the expression of *CEBPα* and *PPARγ* in hMSCs. Expression of *CEBPα* and *PPARγ* was detected by RT-PCR in cells transfected with (*siControl* + *siControl*), (*siControl* + *siCITED2*), (*siControl* + *siSUV39H1*), or (*siCITED2* + *siSUV39H1*) at Day 3, 5, and 7 post-AIM initiation. Expression of each gene was normalized against the expression level of HSP90 and graphed relative to its expression level in (*siControl* + *siControl*). Data were derived from the average of three independent experimental replicates.

respectively, which were approximate to the sum of their fold increases in (*siControl* + *siCITED2*) and (*siControl* + *siSUV39H1*), at 6.45-fold and 12.34-fold, respectively, for *CEBPα*, and 2.23-fold and 3.15-fold, respectively, for *PPARγ*. Taken together, the above results indicated that mirroring its additive effect on the adipogenic differentiation efficiency of hMSCs, co-knockdown of SUV39H1 and CITED2 also exerted cumulative effect on upregulating the expression of *CEBPα* and *PPARγ*.

CEBPα *mediates the effect of* siSUV39H1 *on promoting adipogenesis*

To further confirm that *CEBPα* indeed played a critical role in mediating the effect of *siSUV39H1* on adipogenic differentiation of hMSCs, hMSCs were transfected with (*siControl* + *siControl*), (*siControl* + *siSUV39H1*), or (*siCEBPα* + *siSUV39H1*), and AIM treatment was initiated at 24 h post-transfection, followed by media change at 48-h intervals. Cells were analyzed at Day 14 postadipogenic induction.

As expected, there was stronger OilRedO stain intensity in (*siControl* + *siSUV39H1*) treatment group compared with (*siControl* + *siControl*) control group as shown previously, but the intensity in (*siCEBPα* + *siSUV39H1*) treatment group was reduced to about the same level as in (*siControl* + *siControl*) control (Fig. 8a). Consistently, quantification of fat accumulation by OilRedO dye extraction in (*siControl* + *siSUV39H1*) increased to 159% of (*siControl* + *siControl*), or 1.59-fold increase, but in (*siCEBPα* + *siSUV39H1*) the level was reduced to 107% of (*siControl* + *siControl*) (Fig. 8b). Similarly, percentage of adipocytes in (*siControl* + *siSUV39H1*) increased to 251 of (*siControl* + *siControl*), but reduced significantly in (*siCEBPα* + *siSUV39H1*) to 87 of (*siControl* + *siControl*) (Fig. 8c). To confirm expression knockdown of *CEBPα* by *siCEBPα*, RT-PCR was carried out in cell samples isolated at Day 3 postadipogenic initiation, and expression was normalized against the expression level of internal control gene *HSP90*. While there was a 4.13-fold increase of *CEBPα* expression in (*siControl* + *siSUV39H1)* over (*siControl* + *siControl)* control, expression was reduced by 14.28-fold in (*siCEBPα* + *siSUV39H1)* to 7% of the level in (*siControl* + *siControl)* control (Fig. 8d). The above results demonstrated that CEBPα indeed played a critical role in mediating the effect of *siSUV39H1* on promoting adipogenesis, as such effect was almost completely abolished by the reduction of *CEBPα* expression induced by *siCEBPα*.

Conclusion

In summary, we present evidence that expression knockdown of SUV39H1, a H3K9 histone methyltransferase, *by siSUV39H1*, promoted adipogenic differentiation of hMSCs through both accelerated adipogenesis and increased adipogenic commitment by potentiating individual hMSCs that normally do not respond to AIM to undergo differentiation, whereas expression knockdown of CITED2, a transcriptional

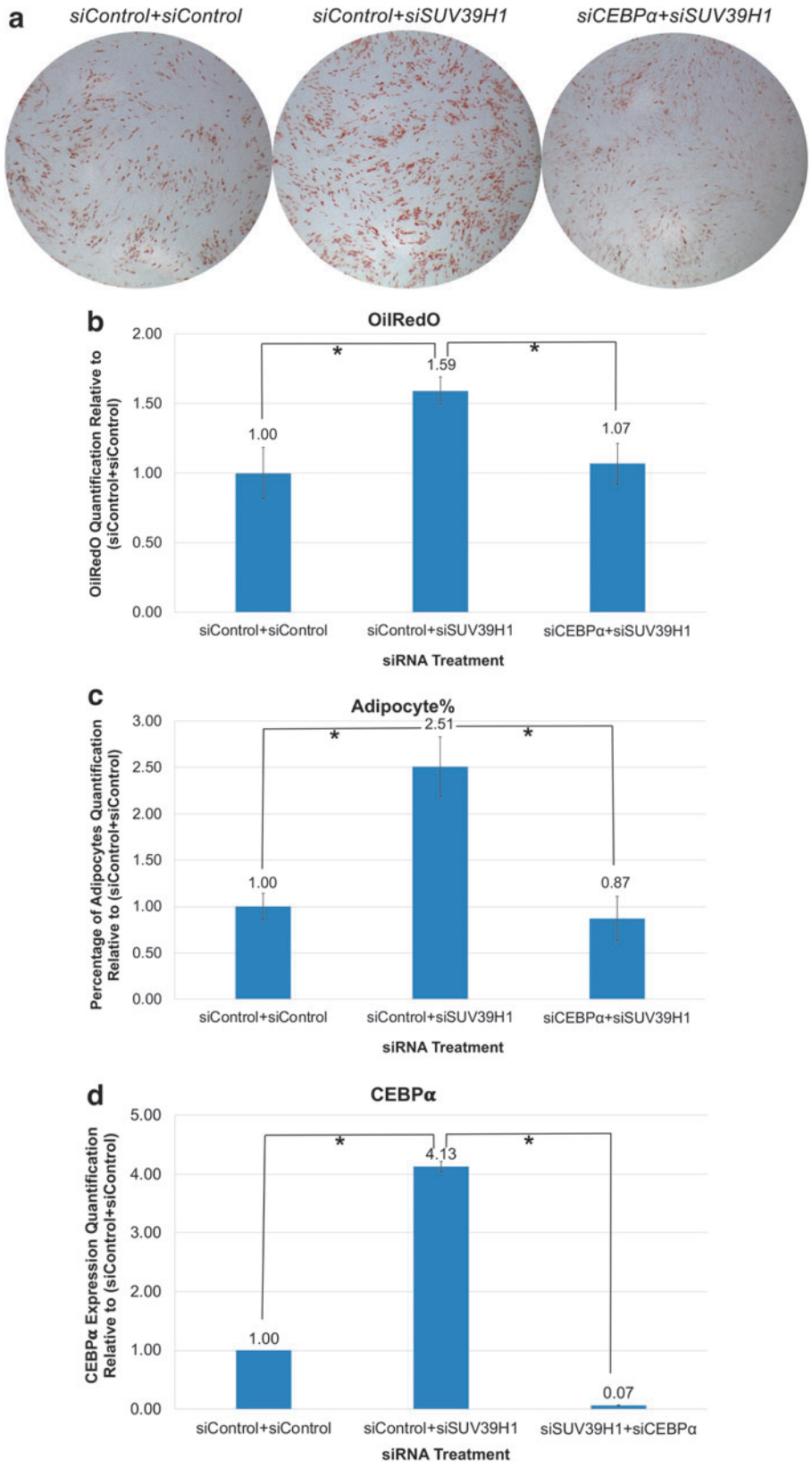

FIG. 8. CEBPα played critical role in mediating the effect of *siSUV39H1* on promoting adipogenesis. HMSCs were transfected with (*siControl* + *siControl*), (*siControl* + *siSUV39H1*), or (*siCEBPα* + *siSUV39H1*), followed by 14 days of AIM treatment. **(a)** Representative whole well images of cells stained with OilRedO; **(b)** OilRedO quantification relative to the level in (*siControl* + *siControl*) control based on the average of three independent experimental replicates; **(c)** percentage of adipocytes quantification relative to the level in (*siControl* + *siControl*) control based on the average of three independent experimental replicates; **(d)** expression of *CEBPα* was detected by RT-PCR at Day 3 post-AIM initiation and graphed relative to its expression level in (*siControl* + *siControl*) after normalization against the expression level of HSP90. $*P < 0.01$.

coregulator, *by siCITED2*, promoted adipogenic differentiation of hMSCs largely through augmented adipogenic commitment only. Furthermore, simultaneous knockdown of both genes resulted in a cumulative effect in enhancing the percentage of cells committing to adipogenesis, at least partly by exerting a cumulative effect on upregulating the expression of both *CEBPα* and *PPARγ*. We also demonstrated the following: (I) the effect of *siSUV39H1* on promoting adipogenesis was independent of the growth media type used to constitute the AIM; (II) both SUV39h1 and

CITED2 were significantly downregulated within the first 24 h of adipogenic induction and remained at a low level of expression afterward during normal differentiation of hMSCs induced by AIM alone; (III) expression knockdown of SUV39H1 and CITED2 strongly inhibited osteogenic differentiation but promoted adipogenic differentiation of hMSCs under osteogenic induction condition; and (IV) CEBPα played a critical role in mediating the effect of *siSUV39H1* on promoting adipogenesis, as such effect was almost completely abolished by cotransfection of *siCEBPα*.

Discussion

During normal adipogenic differentiation, with appropriate stimuli such as phosphodiesterase inhibitor and adenosine receptor antagonist IBMX and glucocorticoid DEX, expression of C/EBPβ and C/EBPδ was rapidly induced, activating the two key transcription factors CEBPα and PPARγ, which subsequently regulate expression of each other through a positive feedback loop and commit some cells to become adipocyte [6,7,47,48]. CEBPα and PPARγ are considered master regulators of adipogenesis and play decisive roles in adipogenic cell fate determination, due to the fact that overexpression of either CEBPα or PPARγ can stimulate adipogenic differentiation from mouse fibroblasts, 3T3-L1, and MSCs [8,49–52].

In this study, single knockdown of SUV39H1 by *siSUV39H1* or CITED2 by *siCITED2* remarkably enhanced adipogenic differentiation efficiency of hMSCs by increasing the percentage of cells becoming mature adipocytes as compared with *siControl* controls without affecting the average cell size of mature adipocytes. The interesting questions were as follows: Why did some cells that did not respond to AIM induction alone commit to adipogenic lineage in the presence of *siSUV39H1* or *siCITED2*? Did CEBPα and/or PPARγ play an important role? Our past study demonstrated that during adipogenic differentiation of hMSCs, cells undergo 4 distinct stages of development post-adipogenic initiation (D0): mitotic phase (D0–D2), growth arrest phase (D2–D3), commitment phase (D3–D6), and lipogenesis phase (after D6) [41]. During the commitment phase, expression of CEBPα and PPARγ soared in AIM-treated cells and represented a pivotal event that tipped the cells' commitment toward adipogenic lineage [41]. Results from this study revealed that expression of CEBPα and PPARγ in *siSUV39H1*- or *siCITED2*-transfected cells was indeed significantly increased as compared with *siControl* controls during the adipogenic commitment stage. Furthermore, expression knockdown of CEBPα nearly abolished the adipogenic enhancement effect induced by *siSUV39H1*, which further supports that the increased expression level of CEBPα did play a critical role in elevating some cells' capacity to commit to adipogenic lineage in the presence of *siSUV39H1*.

How did change in SUV39H1 and CITED2 expression lead to the expression change in CEBPα and PPARγ? Expression knockdown of SUV39H1 by *siSUV39H1* might have altered the expression of both CEBPα and PPARγ through direct regulation of their promoter activity. The promoters of both CEBPα and PPARγ have been shown to undergo H3K9 methylation, which inhibits their expression [25]. In 3T3-L1 preadipocytes, SUV39H1 was shown to methylate H3K9me2 to form H3K9me3, which repressed the expression of CEBPα along with AP-2α [29]. A recent study demonstrated that SUV39H1 could bind to RNA and might achieve its promoter target specificity by binding to chromatin-bound RNAs [53]. These H3K9 methylations may prevent CEBPα and PPARγ from reaching a threshold level to prime cells for adipogenic commitment. In this study, we demonstrated that during normal adipogenic differentiation of hMSCs induced by AIM, expression of SUV39H1 sharply declined within the first 48 h of AIM induction, the mitotic phase, and remained at the same low level thereafter when cell proliferation is arrested, indicating that SUV39H1 expression may be inversely linked to cellular proliferation. Furthermore, downregulation of SUV39H1 clearly preceded the elevated expression of CEBPα and PPARγ during the D3–D6 adipogenic commitment phase and further knockdown of SUV39H1 by *siSUV39H1* led to even greater levels of CEBPα and PPARγ expression, demonstrating that SUV39H1 expression in hMSCs is closely linked to CEBPα and PPARγ expression in an inversed relationship. Based on what is known in 3T3L1 cells, one could reasonably speculate that SUV39H1 also controls expression of CEBPα and PPARγ by regulating their H3K9 methylation levels, with lower expression level of SUV39H1 leading to lower levels of H3K9me3, greater transcriptional activation, higher expression levels of *CEBPα* and *PPARγ*, and hence greater number of cells committing to adipogenic lineage.

Limited evidence is found in the literature, however, that links CITED2 directly to the regulation of *CEBPα* and *PPARγ* promoter activity. Rather, CITED2 may be involved in such regulation through its coregulators. During fetal lung development in mice, CITED2 was found to be present on the *CEBPα* promoter by forming a complex with TCFAP2c [54]. In addition, both p300 and CBP, two known coactivators of CITED2, were found to be indispensable for adipogenic differentiation as adipogenesis was largely suppressed in 3T3-L1 cells expressing p300- or CBP-specific ribozymes and in adipose-specific p300/CBP double knockout mice [33,55], and in 3T3-L1, AP-2α, another CITED2-interacting protein, acts as a repressor of adipogenesis by repressing CEBPα expression [34]. In this study, we demonstrated that during normal adipogenic differentiation of hMSCs induced by AIM, expression of CITED2 sharply declined within the first 24 h of AIM induction, and remained at the same low level, thereafter, indicating that CITED2 expression may be inversely linked to cellular proliferation. Indeed, CITED2 was known to be a regulator of cellular proliferation, and its overexpression led to tumor formation in nude mice [56,57]. Furthermore, downregulation of CITED preceded the elevated expression of CEBPα and PPARγ during the D3–D6 adipogenic commitment phase, and further knockdown of CITED2 by *siCITED2* led to even greater levels of CEBPα and PPARγ expression, demonstrating that, similar to SUV39H1, CITED2 expression in hMSCs is closely linked to CEBPα and PPARγ expression in an inversed relationship. While the mode of action by CITED2 is not clear, one might speculate that it may be linked with histone acetylation modulation through the histone acetyltransferase (HAT) or histone deacetylase (HDAC) activity of its associated proteins. Both CBP and p300 are coactivators containing intrinsic HAT activity

(H3K27) and can also recruit additional HATs to target genes' promoter regions [37]. CITED2 was also shown to interact with GCN5, also a HAT protein, in regulating the activity of PGC-1a and gluconeogenesis during fasting [38,39]. In addition, CITED2 interacted with HDAC1 to potentiate the MYC–HDAC1 complex formation to suppress downstream gene expression including $p21^{CIP1}$ [40]. How CITED2 may be targeted to specific promoter regions such as those of *CEBPα* and *PPARγ*, and with what partners, will be of interest for future studies.

Interestingly, our study demonstrated that simultaneous knockdown of SUV39H1 and CITED2 induced by *siSUV39H1* and *siCITED2,* respectively, exerted an additive effect on the increase of percentage of adipocytes as well as on the upregulation of *CEBPα* and *PPARγ* expression. In other words, in the (*siCITED2* + *siSUV39H1*) co-knockdown cells, the effects of each individual knockdown were combined in an additive manner to result in yet higher percentage of adipocytes and greater expression levels of *CEBPα* and *PPARγ* than either of the single knockdown, (*siControl* + *siCITED2*) or (*siControl* + *siSUV39H1*). Since total cell numbers in (*siCITED2* + *siSUV39H1*) were not statistically significantly different from those in (*siControl* + *siCITED2*) or (*siControl* + *siSUV39H1*), the additive nature of the increase in adipocyte percentage in (*siCITED2* + *siSUV39H1*) co-knockdown as compared with the single knockdowns suggests that *siCITED2* and *siSUV39H1* might have enabled distinct subpopulations of cells that are normally not capable of committing to adipogenic cell fate in response to AIM alone to commit to adipogenic cell fate. This scenario would also help explain the additive nature of the fold increases in *CEBPα* and *PPARγ* expression in (*siCITED2* + *siSUV39H1*) co-knockdown vs. single knockdowns. Since the *siRNA* transfection efficiency is >85% [4,58], this scenario would also suggest that the hMSCs cell culture is heterogeneous. In fact, the heterogeneity of hMSCs cell culture is not something new. While majority of these cells (≥90%) are characterized by the expression of cell surface markers including CD90, CD150, and CD73, only ~8% of cells are capable of clonogenic expansion, and the percentage of cells capable to committing to adipogenic differentiation in response to AIM is usually in the 20–30 range [58]. How distinct subpopulations of cells respond to SUV39H1 and CITED2 knockdown differently would be an area of interest for future study.

Knockdown of *SUV39H1* by *siSUV39H1* also significantly accelerated the process of adipogenesis in some cells. While the percentage of adipocytes increased significantly from Day 14 to Day 30 and remained stable thereafter in both *siControl* and *siCITED2*-treated cells, the percentage of adipocytes in *siSUV39H1*-treated cells did not change significantly from Day 14 to Day 60, indicating that in the former groups, it took some cells >14 days to commit and reach visually recognizable mature adipocyte stage, whereas in the latter group all cells capable of committing to adipogenic lineage were able to commit and reach visually recognizable mature adipocyte stage by Day 14. Interestingly, cell size measurement of individual adipocytes based on stained oil droplets showed that the average cell size was smaller in *siSUV39H1* ($P < 0.02$) and *siCITED2* ($P = 0.0685$) treatment groups as compared with *siControl*, indicating that some committed cells had less fat accumulation in the former groups. Considering that *siSUV39H1* also significantly accelerated the process of adipogenesis in some cells, the two phenomena appear contradictory with each other. However, since the adipocyte percentage in *siSUV39H1* treatment group was 2.44-fold of that in *siControl* control by Day 14, it indicated that majority of the cells committed to adipocytes in *siSUV39H1*-treated cells were cells that normally would not have committed to adipogenic lineage at that point and additionally, cells that would have committed to adipogenic lineage but would not have accumulated sufficient oil droplets to be visually recognizable as mature adipocytes. Hence, it is conceivable that for those majority committed cells, their average fat accumulation was significantly lower than those in cells that normally would have committed and progressed to mature adipocytes in response to AIM alone by Day 14, resulting in an overall lower average cell size measurement in *siSUV39H1* adipocytes than in *siControl* adipocytes. As such, the two phenomena, accelerated adipogenic commitment and smaller adipocyte cell size by Day 14, are not necessarily contradictory to each other and can coexist. The discrepancy in adipocyte cell size between *siSUV39H1/siCITED2* and *siControl* that was observed at Day 14 was no longer present by Day 60, indicating that normal lipogenesis was not compromised in either *siSUV39H1*- or *siCITED2*-transfected cells.

Acknowledgments

We thank laboratory members Julian Aragon and Jacqueline Gutierrez for their technical support.

Author Disclosure Statement

The authors declare no conflict of interest.

Funding Information

This work was supported by NIH grant no. 1SC3GM116720-01 awarded to YX Zhao. No additional external funding was received for this study.

Supplementary Material

Supplementary Table S1
Supplementary Table S2
Supplementary Figure S1
Supplementary Figure S2
Supplementary Figure S3
Supplementary Figure S4

References

1. Arner P and KL Spalding. (2010). Fat cell turnover in humans. Biochem Biophys Res Commun 396:101–104.
2. Green H and M Meuth. (1974). An established preadipose cell line and its differentiation in culture. Cell 3: 127–133.
3. Cristancho AG and MA Lazar. (2011). Forming functional fat: a growing understanding of adipocyte differentiation. Nat Rev Mol Cell Biol 12:722–734.
4. Zhao Y and S Ding. (2007). A high-throughput siRNA library screen identifies osteogenic suppressors in human mesenchymal stem cells. Proc Natl Acad Sci U S A 104: 9673–9678.

5. Qian SW, X Li, YY Zhang, HY Huang, Y Liu, X Sun and QQ Tang. (2010). Characterization of adipocyte differentiation from human mesenchymal stem cells in bone marrow. BMC Dev Biol 10:47.
6. Wu Z, ED Rosen, R Brun, S Hauser, G Adelmant, AE Troy, C McKeon, GJ Darlington and BM Spiegelman. (1999). Cross-regulation of C/EBP alpha and PPAR gamma controls the transcriptional pathway of adipogenesis and insulin sensitivity. Mol cell 3:151–158.
7. MacDougald OA and MD Lane. (1995). Transcriptional regulation of gene expression during adipocyte differentiation. Annu Rev Biochem 64:345–373.
8. Tontonoz P, E Hu and BM Spiegelman. (1994). Stimulation of adipogenesis in fibroblasts by PPAR gamma 2, a lipid-activated transcription factor. Cell 79:1147–1156.
9. Freytag SO, DL Paielli and JD Gilbert. (1994). Ectopic expression of the CCAAT/enhancer-binding protein alpha promotes the adipogenic program in a variety of mouse fibroblastic cells. Genes Dev 8:1654–1663.
10. Peltz L, J Gomez, M Marquez, F Alencastro, N Atashpanjeh, T Quang, T Bach and Y Zhao. (2012). Resveratrol exerts dosage and duration dependent effect on human mesenchymal stem cell development. PLoS One 7: e37162.
11. Ong WK and S Sugii. (2013). Adipose-derived stem cells: fatty potentials for therapy. Int J Biochem Cell Biol 45: 1083–1086.
12. Tran TT and CR Kahn. (2010). Transplantation of adipose tissue and stem cells: role in metabolism and disease. Nat Rev Endocrinol 6:195–213.
13. Aagaard L, G Laible, P Selenko, M Schmid, R Dorn, G Schotta, S Kuhfittig, A Wolf, A Lebersorger, et al. (1999). Functional mammalian homologues of the Drosophila PEV-modifier Su(var)3–9 encode centromere-associated proteins which complex with the heterochromatin component M31. EMBO J 18:1923–1938.
14. Peters AH, S Kubicek, K Mechtler, RJ O'Sullivan, AA Derijck, L Perez-Burgos, A Kohlmaier, S Opravil, M Tachibana, et al. (2003). Partitioning and plasticity of repressive histone methylation states in mammalian chromatin. Mol Cell 12:1577–1589.
15. Black JC and JR Whetstine. (2013). Tipping the lysine methylation balance in disease. Biopolymers 99:127–135.
16. Peters AH, JE Mermoud, D O'Carroll, M Pagani, D Schweizer, N Brockdorff and T Jenuwein. (2002). Histone H3 lysine 9 methylation is an epigenetic imprint of facultative heterochromatin. Nat Genet 30:77–80.
17. Tamaru H and EU Selker. (2001). A histone H3 methyltransferase controls DNA methylation in *Neurospora crassa*. Nature 414:277–283.
18. Lachner M, D O'Carroll, S Rea, K Mechtler and T Jenuwein. (2001). Methylation of histone H3 lysine 9 creates a binding site for HP1 proteins. Nature 410:116–120.
19. Sims RJ, 3rd, K Nishioka and D Reinberg. (2003). Histone lysine methylation: a signature for chromatin function. Trends Genet 19:629–639.
20. Nielsen SJ, R Schneider, UM Bauer, AJ Bannister, A Morrison, D O'Carroll, R Firestein, M Cleary, T Jenuwein, RE Herrera and T Kouzarides. (2001). Rb targets histone H3 methylation and HP1 to promoters. Nature 412:561–565.
21. Vandel L, E Nicolas, O Vaute, R Ferreira, S Ait-Si-Ali and D Trouche. (2001). Transcriptional repression by the retinoblastoma protein through the recruitment of a histone methyltransferase. Mol Cell Biol 21:6484–6494.
22. Vaute O, E Nicolas, L Vandel and D Trouche. (2002). Functional and physical interaction between the histone methyl transferase Suv39H1 and histone deacetylases. Nucleic Acids Res 30:475–481.
23. Okamura M, T Inagaki, T Tanaka and J Sakai. (2010). Role of histone methylation and demethylation in adipogenesis and obesity. Organogenesis 6:24–32.
24. Cho YW, S Hong, Q Jin, L Wang, JE Lee, O Gavrilova and K Ge. (2009). Histone methylation regulator PTIP is required for PPARgamma and C/EBPalpha expression and adipogenesis. Cell Metab 10:27–39.
25. Matsumura Y, R Nakaki, T Inagaki, A Yoshida, Y Kano, H Kimura, T Tanaka, S Tsutsumi, M Nakao, et al. (2015). H3K4/H3K9me3 bivalent chromatin domains targeted by lineage-specific DNA methylation pauses adipocyte differentiation. Mol Cell 60:584–596.
26. Wang L, S Xu, JE Lee, A Baldridge, S Grullon, W Peng and K Ge. (2013). Histone H3K9 methyltransferase G9a represses PPARgamma expression and adipogenesis. EMBO J 32:45–59.
27. Musri MM, MC Carmona, FA Hanzu, P Kaliman, R Gomis and M Parrizas. (2010). Histone demethylase LSD1 regulates adipogenesis. J Biol Chem 285:30034–30041.
28. Czvitkovich S, S Sauer, AH Peters, E Deiner, A Wolf, G Laible, S Opravil, H Beug and T Jenuwein. (2001). Overexpression of the SUV39H1 histone methyltransferase induces altered proliferation and differentiation in transgenic mice. Mech Dev 107:141–153.
29. Zhang ZC, Y Liu, SF Li, L Guo, Y Zhao, SW Qian, B Wen, QQ Tang and X Li. (2014). Suv39h1 mediates AP-2alpha-dependent inhibition of C/EBPalpha expression during adipogenesis. Mol Cell Biol 34:2330–2338.
30. Yin Z, J Haynie, X Yang, B Han, S Kiatchoosakun, J Restivo, S Yuan, NR Prabhakar, K Herrup, et al. (2002). The essential role of Cited2, a negative regulator for HIF-1alpha, in heart development and neurulation. Proc Natl Acad Sci U S A 99:10488–10493.
31. Braganca J, JJ Eloranta, SD Bamforth, JC Ibbitt, HC Hurst and S Bhattacharya. (2003). Physical and functional interactions among AP-2 transcription factors, p300/CREB-binding protein, and CITED2. J Biol Chem 278:16021–16029.
32. Bhattacharya S, CL Michels, MK Leung, ZP Arany, AL Kung and DM Livingston. (1999). Functional role of p35srj, a novel p300/CBP binding protein, during transactivation by HIF-1. Genes Dev 13:64–75.
33. Takahashi N, T Kawada, T Yamamoto, T Goto, A Taimatsu, N Aoki, H Kawasaki, K Taira, KK Yokoyama, Y Kamei and T Fushiki. (2002). Overexpression and ribozyme-mediated targeting of transcriptional coactivators CREB-binding protein and p300 revealed their indispensable roles in adipocyte differentiation through the regulation of peroxisome proliferator-activated receptor gamma. J Biol Chem 277:16906–16912.
34. Jiang MS, QQ Tang, J McLenithan, D Geiman, W Shillinglaw, WJ Henzel and MD Lane. (1998). Derepression of the C/EBPalpha gene during adipogenesis: identification of AP-2alpha as a repressor. Proc Natl Acad Sci U S A 95:3467–3471.
35. Chou YT, H Wang, Y Chen, D Danielpour and YC Yang. (2006). Cited2 modulates TGF-beta-mediated upregulation of MMP9. Oncogene 25:5547–5560.

36. van Zoelen EJ, I Duarte, JM Hendriks and SP van der Woning. (2016). TGFbeta-induced switch from adipogenic to osteogenic differentiation of human mesenchymal stem cells: identification of drug targets for prevention of fat cell differentiation. Stem Cell Res Ther 7:123.
37. Vo N and RH Goodman. (2001). CREB-binding protein and p300 in transcriptional regulation. J Biol Chem 276: 13505–13508.
38. Sakai M, T Tujimura-Hayakawa, T Yagi, H Yano, M Mitsushima, H Unoki-Kubota, Y Kaburagi, H Inoue, Y Kido, M Kasuga and M Matsumoto. (2016). The GCN5-CITED2-PKA signalling module controls hepatic glucose metabolism through a cAMP-induced substrate switch. Nat Commun 7:13147.
39. Sakai M, M Matsumoto, T Tujimura, C Yongheng, T Noguchi, K Inagaki, H Inoue, T Hosooka, K Takazawa, et al. (2012). CITED2 links hormonal signaling to PGC-1alpha acetylation in the regulation of gluconeogenesis. Nat Med 18:612–617.
40. Chou YT, CH Hsieh, SH Chiou, CF Hsu, YR Kao, CC Lee, CH Chung, YH Wang, HS Hsu, et al. (2012). CITED2 functions as a molecular switch of cytokine-induced proliferation and quiescence. Cell Death Differ 19:2015–2028.
41. Marquez MP, F Alencastro, A Madrigal, JL Jimenez, G Blanco, A Gureghian, L Keagy, C Lee, R Liu, et al. (2017). The role of cellular proliferation in adipogenic differentiation of human adipose tissue-derived mesenchymal stem cells. Stem Cells Dev 26:1578–1595.
42. Carpenter AE, TR Jones, MR Lamprecht, C Clarke, IH Kang, O Friman, DA Guertin, JH Chang, RA Lindquist, et al. (2006). CellProfiler: image analysis software for identifying and quantifying cell phenotypes. Genome Biol 7:R100.
43. Zhang Y, D Khan, J Delling and E Tobiasch. (2012). Mechanisms underlying the osteo- and adipo-differentiation of human mesenchymal stem cells. Sci World J 2012:793823.
44. Grigoriadis AE, JN Heersche and JE Aubin. (1988). Differentiation of muscle, fat, cartilage, and bone from progenitor cells present in a bone-derived clonal cell population: effect of dexamethasone. J Cell Biol 106:2139–2151.
45. Filippi-Chiela EC, MM Oliveira, B Jurkovski, SM Callegari-Jacques, VD da Silva and G Lenz. (2012). Nuclear morphometric analysis (NMA): screening of senescence, apoptosis and nuclear irregularities. PLoS One 7: e42522.
46. Beresford JN, JH Bennett, C Devlin, PS Leboy and ME Owen. (1992). Evidence for an inverse relationship between the differentiation of adipocytic and osteogenic cells in rat marrow stromal cell cultures. J Cell Sci 102 (Pt 2): 341–351.
47. Lowe CE, S O'Rahilly and JJ Rochford. (2011). Adipogenesis at a glance. J Cell Sci 124:2681–2686.
48. Cristancho AG and MA Lazar. (2011). Forming functional fat: a growing understanding of adipocyte differentiation. Nat Rev Mol Cell Biol 12:722–734.
49. Sheyn D, G Pelled, W Tawackoli, S Su, S Ben-David, D Gazit and Z Gazit. (2013). Transient overexpression of Ppargamma2 and C/ebpalpha in mesenchymal stem cells induces brown adipose tissue formation. Regen Med 8: 295–308.
50. Yuan SM, Y Guo, Q Wang, Y Xu, M Wang, HN Chen and WM Shen. (2017). Over-expression of PPAR-gamma2 gene enhances the adipogenic differentiation of hemangioma-derived mesenchymal stem cells in vitro and in vivo. Oncotarget 8:115817–115828.
51. Qian SW, X Li, YY Zhang, HY Huang, Y Liu, X Sun and QQ Tang. (2010). Characterization of adipocyte differentiation from human mesenchymal stem cells in bone marrow. BMC Dev Biol 10:47.
52. Freytag SO, DL Paielli and JD Gilbert. (1994). Ectopic expression of the CCAAT/enhancer-binding protein alpha promotes the adipogenic program in a variety of mouse fibroblastic cells. Genes Dev 8:1654–1663.
53. Shirai A, T Kawaguchi, H Shimojo, D Muramatsu, M Ishida-Yonetani, Y Nishimura, H Kimura, JI Nakayama and Y Shinkai. (2017). Impact of nucleic acid and methylated H3K9 binding activities of Suv39h1 on its heterochromatin assembly. Elife 6:e25317.
54. Xu B, X Qu, S Gu, YQ Doughman, M Watanabe, SL Dunwoodie and YC Yang. (2008). Cited2 is required for fetal lung maturation. Dev Biol 317:95–105.
55. Tamucci KA, M Namwanje, L Fan and L Qiang. (2018). The dark side of browning. Protein Cell 9:152–163.
56. Kranc KR, SD Bamforth, J Braganca, C Norbury, M van Lohuizen and S Bhattacharya. (2003). Transcriptional coactivator Cited2 induces Bmi1 and Mel18 and controls fibroblast proliferation via Ink4a/ARF. Mol Cell Biol 23: 7658–7666.
57. Sun HB, YX Zhu, T Yin, G Sledge and YC Yang. (1998). MRG1, the product of a melanocyte-specific gene related gene, is a cytokine-inducible transcription factor with transformation activity. Proc Natl Acad Sci U S A 95: 13555–13560.
58. Madrigal A, L Tan and Y Zhao. (2017). Expression regulation and functional analysis of RGS2 and RGS4 in adipogenic and osteogenic differentiation of human mesenchymal stem cells. Biol Res 50:43.

Address correspondence to:
Dr. Yuanxiang Zhao
Biological Sciences Department
California State Polytechnic University at Pomona
3801 W. Temple Avenue
Pomona, CA 91768
USA

E-mail: zhao@cpp.edu

Received for publication November 16, 2020
Accepted after revision March 10, 2021
Prepublished on Liebert Instant Online March 10, 2021